

The Study of Two Dimensional Bluff Body Wake Flows With The Effect Of Underneath Wavy Surface

Asral

Jurusan Teknik Mesin Fakultas Teknik Universitas Riau
Kampus Bina Widya, Km.12,5 Simpang Baru Panam, Pekanbaru
Asral_2008@yahoo.com

ABSTRACT

The present study observes the effect of wave-like structure on flow after a bluff body. Particle Image Velocimetry (PIV) technique has been employed to measure the flow velocity and to capture the flow pattern in various wavy surface conditions, positions of bluff body of which has height to width ratio of two, and Reynolds numbers. Two-dimensional numerical solution for the same test condition has been performed by employing the turbulent model of $RNG k - \epsilon$. Sinusoidal surfaces were chosen for wavy condition to represent the wavy boundary. Range of Reynolds numbers were 1480 to 3300 and the wave amplitudes were 0.13 of the bluff body height (0.13D), 0.33D and 0.67D. Comparisons were made against flow over the flat surface for the same flow condition. For most cases studied, two vortices always present in the region in the vicinity close to the bluff body. Larger size of vortices appears in the upper area than those in the lower area of the flow. For low amplitude wave, the flow tends to follow the wave and resulted in large U-component negative velocity zone behind the bluff body. As the wave amplitude increases, the size of this negative velocity region will reduce. Low amplitude wave also increases the fluctuation of the flow as the Reynolds number increases. However, higher wave amplitude suppresses the flow to the same order of fluctuations. In general, the numerical solutions were in good agreement with the experimental results.

Keywords: PIV, vortex, wave, bluff body

1. INTRODUCTIONS

The profile of flow around bluff bodies such as cubes, rectangular and circular cylinders, and flat plates are relevant to many engineering designs, such as constructions under the action of wind loading like building, chimneys and water tank tower, steel tower suspension bridges or marine structures under the action of water loading. Wind driving forces on infrastructures, located nearby coastal region are considered to be an important parameter in design. The presence of them on the shores is experienced on the wave water in any direction of wind flows. The wind load to the buildings at the coasts can exert from the land and the sea direction. The increase of speed of wind flow magnitudes cause the high amplitude of water wave before exerting the structure. The flow patterns around the structure are different between water wave and over the ground. Since the wind exerting on the structures vortices, this phenomena affects to the structures. It can destructive and risk to the life safety. Because flow vortex detected can create the high energy and cause to collapse the bridges and buildings. So in constructing a structure should be strong enough to decrease the risk caused by the wind. The energy of wind exerting on the structures depend on the direction flow to the cross- area, different direction will give different effect to them (Richard and Hoxey, 2002). The dominant wind loads works as normal to the infrastructure is considered as the main parameter in design process.

The objective of this current study is to investigate the effect of wavy boundaries upon profile of flow after a bluff body for various Reynolds numbers. PIV was used for qualitative visualization, and quantitative of the flow field. These can then be used to analyze the flow using the velocity data determined. This measuring method is a well established quantitative flow visualization technique (Nakagawa and Hanratty (2001), Zhang, Daichin, and Lee (2005), Angele and Klingmann (2006)). The method utilizes techniques of flow visualization whereby the flow is seeded with light scattering particles which are assumed to follow the flow. The plane of interest is illuminated by a sheet of laser light and an image of the in plane movement of the particles recorded. A short duration multiple exposure images of particles are recorded and analyzed to obtain the velocity field.

Experimental study on the characteristics of flow in the wake region of bluff body with the ground effect has been investigated by Kim and Gerops (1998). The author studied the effect of various ground clearances on the flow around a variety of bluff bodies. Barlow *et al.* (2001) presented the ground effect with different aspect ratios, varying ground clearances, and different levels of underbody roughness were performed in wind tunnel experiment. Jeffrey *et al.* (1984) identified the separated region, an attached boundary layer, and a free shear layer formed by the detachment of the boundary layer from the wave surface. Zhang *et al.* (2005) reported the sinusoidal surface geometry significantly modifies the near-wake structure and strongly controls the three-dimensional vortices formed in the near wake. Larose and Auteuil (2006) demonstrated that the aerodynamics of bluff bodies with sharp edges can be sensitive to Reynolds number effects. Schewe (2001) reported that Reynolds-number effects can have drastic consequences on the unsteady behaviour and on the fluid forces acting on an aeroelastic system.

Computational fluid modeling in wake region has been widely used by many researchers in their investigation (Rodi (1997), Bouris and Bergeles (1999), Krajnovic and Davidson (2001)). Selvarajan, Tulapurkara, and Ram (1998) reported the amplitude of shear stress along the wall increases and pressure decreases with increase in Reynolds number.

Nowadays, since computing time is not as expensive as it was decades ago, the role of computer modeling has been part and partial of fluid flow research. Taking these advantages, in this study, numerical approach was used to aid predictions and assist observations for flow conditions after the bluff body.

2. NUMERICAL APPROACH

In principle, the basic equation used in this case study is continuity equations and the momentum equations written as follows:

$$\frac{\partial \rho}{\partial t} + \nabla \cdot (\rho \vec{v}) = S_m \quad (1)$$

$$\frac{\partial}{\partial t} (\rho u_i) + \frac{\partial}{\partial x_j} (\rho u_i u_j) = -\frac{\partial p}{\partial x_i} + \frac{\partial}{\partial x_j} \left[\mu \left(\frac{\partial u_i}{\partial x_j} + \frac{\partial u_j}{\partial x_i} - \frac{2}{3} \delta_{ij} \frac{\partial u_l}{\partial x_l} \right) \right] + \frac{\partial}{\partial x_j} (-\overline{\rho u_i u_j}) \quad (2)$$

The turbulent kinetic energy, k transport equation for The RNG $k - \varepsilon$ model, given by:

$$\frac{\partial}{\partial t} (\rho k) + \frac{\partial}{\partial x_i} (\rho k u_i) = \frac{\partial}{\partial x_j} \left(\alpha_k \mu_{eff} \frac{\partial k}{\partial x_j} \right) + G_k + G_b - \rho \varepsilon - Y_M + S_k \quad (3)$$

and for dissipation rate, ε written by:

$$\frac{\partial}{\partial t} (\rho \varepsilon) + \frac{\partial}{\partial x_i} (\rho \varepsilon u_i) = \frac{\partial}{\partial x_j} \left(\alpha_\varepsilon \mu_{eff} \frac{\partial \varepsilon}{\partial x_j} \right) + C_{1\varepsilon} \frac{\varepsilon}{k} (G_k + C_{2\varepsilon} G_b) - C_{2\varepsilon} \rho \frac{\varepsilon^2}{k} - R_\varepsilon + S_\varepsilon \quad (4)$$

In these equations, G_k represents the generation of turbulence kinetic energy due to the mean velocity gradients. G_b is the generation of turbulence kinetic energy due to buoyancy. Y_M represents the contribution of the fluctuating dilatation in compressible turbulence to the overall dissipation rate. The quantities α_k and α_ε are the inverse effective Prandtl numbers for k and ε , respectively. S_k and S_ε are user-defined source terms. The model constants $C_{1\varepsilon}$ and $C_{2\varepsilon}$ have values derived analytically by the RNG theory. These values, used by default in FLUENT, are:

$$C_{1\varepsilon} = 1.42, \quad C_{2\varepsilon} = 1.68, \quad C_\mu = 0.0845$$

For all test cases Fluent was employed to predict the flow pattern and condition. Two-dimensional model was used to simulate the flow against the bluff body on the wavy surfaces. The flow was simulated in a numerical tunnel. No slip boundary conditions were imposed on all walls. The ratio of the length of the test section to the height of the bluff body is 63. The ratio of the height of the test section to the height of the bluff body is 14.5. The uniform flow conditions at inlet for Reynolds number 1480, 1850, 2775, and 3300 were used in this study. Air is flowing

through the wavy surface from the right and solutions were forced in order to study the characteristic of the vortex in the wake region.

In order to simulate the effect of wavy surface to the flow against the bluff body, sinusoidal surface with different amplitude were used. Flat surface was also included for comparison. The $k-\varepsilon$ model was used to capture the turbulent phenomenon. Intensity of the grid was increased within the area of the vortex. Simulations were left to run until steady state conditions were reached.

3. EXPERIMENTAL SETUP

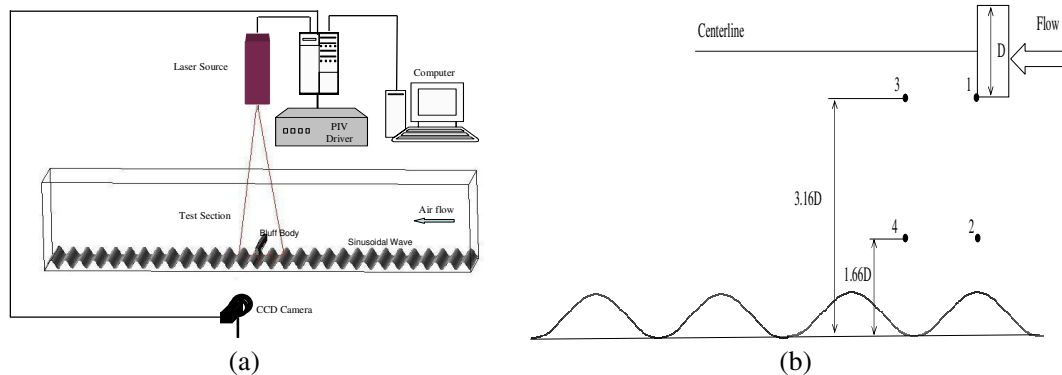


Fig. 1 Schematic diagram of experimental setup and PIV system (a), the bluff body positions setup, and definition of centerline of flow profile (b). Not to scale.

3.1 FLOW SYSTEM

Fig. 1 is a schematic diagram of the experimental setup. The test section of the wind tunnel is 1.89 m long and has 29 cm x 43.5 cm cross-sectional area. To ensure the uniformity of the flow at inlet the honeycomb structure were placed. The flow coming out of the honeycomb then flow over the wavy surfaces and against the bluff body. The amplitudes of wavy surface were 0.33 D , 0.66 D , and 1.3 D , where D is height of the bluff body. The bluff body with 2 x 3 x 29.5 cm in dimension was placed as seen in Fig.1. A gate valve was used to control the flow rate of the air in the tunnel. The mean velocity before the bluff body was set varied from 0.8 m/s, 1 m/s, 1.5 m/s, and 1.8 m/s. The bluff body wake air velocity was measured during each run. The air flow was seeded with smoke of vaporizing fog oil droplet which produces seeding particles on the order 1 μ m in diameter.

3.2 PIV SYSTEM

The experimental technique used in this study for measurement of the velocity is a multiple pulsed photographic system. A simplified diagram of the PIV setup is shown in Fig. 1. A DANTEC Neodymium – YAG laser double pulsing at 10 Hz was used to illuminate the flow field. The Nd-YAG laser source was securely mounted on top of the wind tunnel test section. As shown in the Fig.1, the resulting light sheet illuminated a XY- plane, which inline with the centerline of the body. The illuminated section was imaged using NIKON cross correlation CCD camera having 1200 x 1600 pixels with time interval of 1/1000 sec. the camera was set perpendicular to the test section and right angles to the laser sheet as shown in Fig. 1. The pulsing light sheet and the camera are synchronized so that particle positions at the instant of light pulsed number 1 are registered on frame 1 of the camera and particle positions of light pulse number 2 are registered on frame 2 of the camera. A FlowMap which is dedicated software for DANTEC PIV system was used for data acquisition and processing. The experimental data obtained was recorded in the computer and analyzed using FlowManager software which provides fast data capture, evaluation, and display. The meaningful visual representation of velocity field vector map and streamline were also done by this software.

4. RESULTS AND DISCUSSION

In this section, tabulated data of characteristics of the flow for various Reynolds numbers will be discussed. The characterizations are based on the following definition.

- i) Region of negative U-component velocities behind the bluff body- this region is defined as the major activity that occurred behind the bluff body. Volatile flow in this region can affect the variation of drag coefficient for the bluff body. Vortex could be present in this region. Similar characterization has been used by Johansen, Wu, and Shyy (2004).
- ii) Overall bandwidth measured with referenced to peak positive and negative velocities-this bandwidth is defined as measurement of average fluctuations for U-component and V-component velocities for all flow Reynolds numbers for the same wave. Bigger bandwidth shows rigorous change in direction of flow.
- iii) Fluctuation of velocities with respect to variations of each Reynolds number- this fluctuation is defined as the effect of Reynolds number to the flow.
- iv) Overall downstream velocities approaching main velocity-this characteristic defines the behavior of the flow at further downstream as it merged into the main stream flow. High gradient means the flow is approaching the main stream at a faster rate and low gradient means otherwise.

4.1 Flat Surface

Moving the bluff body vertically closer to the flat surface showed region of backflow is in the same order of magnitude. High Reynolds number seemed to produce the smallest region. On the other hand, Johansen, Wu, and Shyy (2004) showed backflow region was reduced in size. Also, the overall flow seemed to be reduced in bandwidth. As the bluff body approached the ground, the flow took longer time to merge with the main flow. Larger fluctuation was observed for low Reynolds number when the body was further away, but reversed phenomena were seen at higher Reynolds number.

4.2 Wave-1

These case studies were intended to study the effect of wavy surface on the flow behavior. Wave-1 which was a small amplitude wave with slightly sloped surface was observed to change the flow behavior. In comparison for four positions where the bluff body located above the peak and the valley of the wave, the size of the region of negative backward flow increased fifty percents as compared to that of flat surface. Again, the size of the region of backward flow was inversely related to Reynolds number, above the peak of wave increased Reynolds number the region becomes smaller for position furthest the wave and larger for position closer to the wave. However for position above the valley is in the contrary. The bandwidth remained to be in the same order. When it is compared to the flat surface, in wave-1 appeared the difference magnitude of the peak of velocity. This result indicated the wavy surface could affect the behavior of flow along the centerline. For the bluff body closer to the wave, the bandwidth becomes smaller and tend to increase compared to the flat surface. High Reynolds number produced high fluctuation for body close and further away from the wave as compared to that of low Reynolds number. Comparing the four positions, position 1 had the larger fluctuation. However, the downstream flow for position 3 seemed to merge into mainstream at earlier time than that of position 1, 2, and 4.

4.3 Wave-2

In the present study the effect of increased of wave amplitude was studied. Wave-2, which had amplitude larger than that of wave-1, was imposed to observe the change of flow behavior. In comparison of four positions where the bluff body was located above the peak and the valley of the wave, the size of the region of negative backward flow showed decreased half in size as compared to that of wave-1, even though the amplitude of wave-2 was double of wave-1. When the bluff body was located closest to the wave (position 2 and position 4), the region of negative velocity showed greater region for position 4. This is due to the fact that the flow after the bluff

body was affected by the peak of the wave that it encountered right after the bluff body. On the other hand, flow for position 2 encountered a trough right after the bluff body. This result indicated that in wave-2 the effect of the wavy surface to the flow behavior appeared to be more significant as compared to that in wave-1. As the bluff body moved further vertically upward (position 1 and position 3), the negative region of the flow was seemed to be in the same order of magnitude but both were lower than that of position 4 and higher than that of position 2. These results show that the effect of wave is diminishing but still present and will eventually reach size of $1D$ as discussed by Johansen, Wu and Shyy (2004). According to Nakayama and Sakio (2002), the flow took about twice the amplitude of the wave to reach free stream velocity from the trough. In this study, even though the location of the bluff body was outside the range discussed by Nakamaya and Sakio (2002), the results still showed the effect of the wavy surface. For this case, the bandwidth increased in both locations as it moved further upward (position 2 to position 1 and position 4 to position 3). Comparing the results of wave-2 with that of wave-1, the latter wave showed smaller bandwidth. This shows that the increase in wave amplitude suppresses the fluctuations of flow for all Reynolds number studied. For location further upward from the wave (position 1 and position 3), the amplitude of the waves showed no significant effect to the fluctuation of the flow.

At position 1, the fluctuation of the flow decreased as the Reynolds number increased. However, as the bluff body moved closer the wave (position 2), the relationship was otherwise. For position 3, the flow again showed decreased in fluctuations as the Reynolds numbers increased but no significant changes in fluctuation for position 4 as the Reynolds numbers were varied. Meanwhile, the downstream flow for position 3 seemed to reach the mainstream velocity the earliest and followed by position 1, 4, and 2. This means that when the bluff body is located further upward, it seemed to settle down earlier as compared to that of position closer to the wave.

4.4 Wave-3

Further increasing the amplitude of wave to approximately $1.3D$ showed further changes to the flow behavior. Firstly, the region of negative velocity reduced drastically to approximately 20 percent of its size when moving from position 1 (highest) to position 2 (lowest) when the bluff body is above the crest of the wave. Less drastic reduction was observed when bluff body moved from position 3 (highest) to position 4 (lowest) when the bluff body was placed above the trough. For the locations of bluff body above the crest and the trough of the wave, the region of negative velocity seemed to increase. This shows that, the amplitude of the wave has significant effect on the behavior of the flow right after the bluff body. All results are valid for all Reynolds numbers studied. Secondly, comparing the bandwidths of all flow conditions showed that for the same horizontal position of the bluff body, the bandwidths maintained its magnitude but the magnitude reduced as the bluff body moved vertically closer to the wave, i.e. approximately 70 percent. Larger fluctuation was observed for flow with low Reynolds number when the body was further away, but reversed phenomena were seen at flow with higher Reynolds number. However, no significant effect by Reynolds number to the flow fluctuation as the bluff body moved vertically closer to the wave. Finally, this case study shows no particular trend is observed with respect to the flow approaching main stream velocity.

The samples of graphical representations of the discussion are shown in Fig. 4 and the summary of the quantitative criteria are tabulated in Table 1 and Table 2.

Flow field after the bluff body was measured by PIV and calculated using numerical solution. Sample results of time-average velocity vector fields are shown in Fig. 2 and Fig. 3. It can be seen that the vortices were found to shed along the shear layer generated from the edge of bluff body. For position 1 where the bluff body placed further from the surface three vortices were visible for experimental and one for numerical. It is possible that the numerical solution may have not been able to capture all the small vortices present.

For position 2, where the bluff body above the crest of the surface, small vortices emerged behind the bluff body. Approximately four to five small vortices were visible for both numerical and experimental results were observed. It is possible that the numerical solution may have not

been able to capture all the small vortices present. The region of formation of vortex took place in a region approximately of $4.3D$ from behind bluff body. It can be seen that the lower vortex (below centerline at the bluff body) are smaller than the upper vortex. Owing to the wave clearance, which limited the amount of fluid that can be entrained by the lower vortex.

For position 3 where the bluff body placed further above the valley of the wave two vortices displayed in the lower area and one in the upper area of the bluff body. Numerically fail to capture the vector same to the experimental results. For position 4 where the bluff body placed closer to the trough of the wave, both of numerical and experimental exhibited three vortices after the bluff body, nonetheless different in location and size.

In this study was investigated closer to the wave, the wavy surface significantly affected the flow fields due to small clearance between the bluff body and the wave.

5. CONCLUSION

The results of this study allow the following conclusions to be drawn:

1. For all cases studied, two vortices appeared in the region in the vicinity close to the bluff body. In some cases only one vortex appeared in this region.
2. Non-symmetrical vertical profiles of the velocities were obtained for flow around bluff body with ground effect as oppose to symmetrical flow for flow around bluff body without ground effect.
3. Flow with tend to follow wave with low amplitude and this results wider size of negative region. As the amplitude increases, the size will reduce.
4. Flow bandwidth was observed to be suppressed as the amplitude of the wave increases. The vertical distance of the bluff body only affect the magnitude of bandwidth.
5. Low amplitude wave was observed to increase the fluctuation of the flow as the Reynolds number increase. However, for higher wave amplitude, variation in Reynolds number yields the same order of fluctuation.

6. REFERENCES

1. Angele, K.P, and Klingmann, B. Muhammad, (2006), "PIV measurements in a weakly separating and reattaching turbulent boundary layer", *European Journal of Mechanics B/Fluids*, 25: 204–222.
2. Ahmed, M.R, and Sharma, S.D., (2005), "An investigation on the aerodynamics of a symmetrical airfoil in ground effect ", *Experimental Thermal and Fluid Science*, 29:633–647.
3. Bentley, J.P., and Mudd, J.W., (2003), "Vortex Shedding Mechanisms in Single and Dual Bluff Bodies", *Flow Measurement and Instrumentation*, 14: 23-31.
4. Barlow, Jewel B., Guterres, Rui and Ranzenbach, Robert., (2001), "Experimental parametric study of rectangular bodies with radiused edges in ground effect", *Journal of Wind engineering and Industrial Aerodynamics*, 89:1291-1309.
5. Bouris, D, and Bergeles, G., (1999), "2D LES of vortex shedding from a square cylinder", *Journal of Wind Engineering and Industrial Aerodynamics*, 80: 31-46.
6. Bearmen, P.W., (1997), "Near Wake Flows Behind Two-and Three-Dimensional Bluff Bodies", *Journal of Wind Engineering and Industrial Aerodynamics*, 69-71: 33-54.
7. Buckles, Jeffrey, Hanratty, Thomas J., and Adrian, Ronald J., (1984), "Turbulent Flow Over Large-Amplitude Wavy Surfaces", *Journal Fluid Mechanics*, 140: 27-44.
8. Jue, Tswen-Chyuan. (2004), "Numerical analysis of vortex shedding behind a porous square cylinder", *International Journal of Numerical Methods for Heat & Fluid Flow*, 14: 5, pp. 649-663.
8. Huang, Rong F., and Lin, Chih L., (2000), "Velocity field of a bluff-body wake", *Journal of Wind Engineering and Industrial Aerodynamics*, 85:31-45.
- Johansen, Stein T., Wu, Jiongyang, and Shyy, Wei., (2004), "Filter-based unsteady RANS computations", *International Journal of Heat and Fluid Flow*, 25:10-21.

9. Kim, M.S, and Geropp. D., (1998), “*Experimental investigation of the ground effect on the flow around some two-dimensional bluff bodies with moving-belt technique*”, Journal of Wind Engineering and Industrial Aerodynamics, 74-76: 511-519.
10. Nakagawa, Shinji and Hanratty, Thomas J., (2001), “Particle image velocimetry measurements of flow over a wavy wall”, Physics of Fluids, 13: 11.
11. Rodi, W., (1997), “*Comparison of LES and RANS calculations of the flow around bluff bodies*”, Journal of Wind Engineering and Industrial Aerodynamics, 69-71: 55-75.
12. Saha, A.K, Biswas, G, and Muralidhar, K., (2003), “*Three-dimensional study of flow past a square cylinder at low Reynolds numbers*”, International Journal of Heat and Fluid Flow, 24:54–66.
13. Williamson, C.H.K., (1997), “*Advances in Our Understanding of Vortex Dynamics in Bluff Body Wakes*”, Journal of Wind Engineering and Industrial Aerodynamics, 69-71: 3-32.
14. Zhang, Wei, Daichin, and Lee, Sang Joon. (2005), “*PIV Measurement of The Near-Wake Behind a Sinusoidal Cylinder*”, Springer-Verlag.10.1007/s00348-005-0981-9.
15. Schewe, Gunter (2001), “*Reynolds-number Effects in Flow Around More-or-Less Bluff Bodies*”, Journal of Wind Engineering and Industrial Aerodynamics. 89: 1267–1289.
16. Selvarajan, S., Tulapurkara, E.G, and Ram, V. Vasanta (1998), “*A Numerical Study of Flow Through Wavy-Walled Channels*”, Int. J. Numer. Meth. Fluids. 26: 519-531.

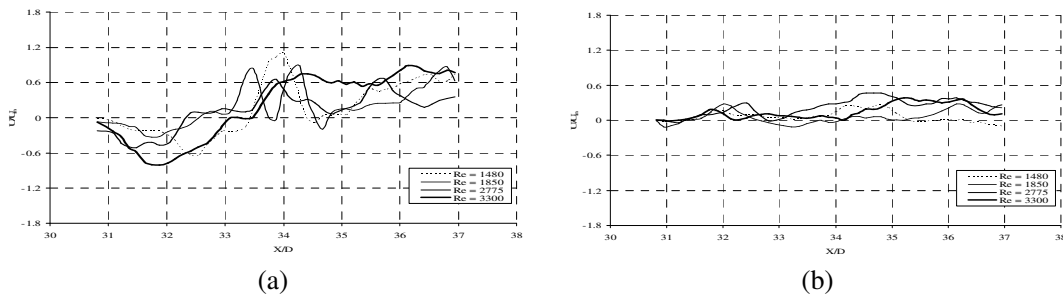


Fig.4 Velocity U-components at centerline in various Reynolds number for wave-3 from experimental, (a) position 1 and (b) position 2.

Table 1: Characteristics of flow for position 1 and position 2 (above the crest of the wave)

| Surfaces | Characteristics of flow | Finding | | |
|----------|----------------------------------------------------------------------------------|----------------------|---------------------|-------|
| | | Position 1 | Position 2 | |
| Flat | Region negative velocities behind the bluff body | 2.6D | 2.4D | |
| | Overall bandwidth measured with reference to peak positive and negative velocity | 1.54U _{in} | 1.4U _{in} | |
| | Overall downstream velocities approaching main velocity | Early | Late | |
| | Fluctuation of velocities with respect to variation of each Reynolds number | Low Reynolds number | Large | Small |
| | | High Reynolds number | Small | Large |
| Wave-1 | Region negative velocities behind the bluff body | 3.7D | 2.6D | |
| | Overall bandwidth measured with reference to peak positive and negative velocity | 1.71U _{in} | 1.46U _{in} | |
| | Overall downstream velocities approaching main velocity | Early | Early | |
| | Fluctuation of velocities with respect to variation of each Reynolds number | Low Reynolds number | Large | Large |
| | | High Reynolds number | Large | Large |
| Wave-2 | Region negative velocities behind the bluff body | 1.86D | 1.53D | |
| | Overall bandwidth measured with reference to peak positive and negative velocity | 1.5U _{in} | 0.72U _{in} | |
| | Overall downstream velocities approaching main velocity | Early | Late | |
| | Fluctuation of velocities with respect to variation of each Reynolds number | Low Reynolds number | Large | Small |
| | | High Reynolds number | Small | Large |
| Wave-3 | Region negative velocities behind the bluff body | 2.6D | 0.53D | |
| | Overall bandwidth measured with reference to peak positive and negative velocity | 1.5U _{in} | 0.48U _{in} | |
| | Overall downstream velocities approaching main velocity | Early | Late | |
| | Fluctuation of velocities with respect to variation of each Reynolds number | Low Reynolds number | Large | Small |
| | | High Reynolds number | Small | Small |

Table 2: Characteristics of flow for position 3 and position 4 (above the trough of the wave)

| Surfaces | Characteristics of flow | Finding | |
|----------------------|----------------------------------------------------------------------------------|---------------------|---------------------|
| | | Position 3 | Position 4 |
| Wave-1 | Region negative velocities behind the bluff body | 3.7D | 2.5D |
| | Overall bandwidth measured with reference to peak positive and negative velocity | 1.7U _{in} | 1.58U _{in} |
| | Overall downstream velocities approaching main velocity | Early | Late |
| | Fluctuation of velocities with respect to variation of each Reynolds number | Low Reynolds number | Small |
| High Reynolds number | | Small | Small |
| Wave-2 | Region negative velocities behind the bluff body | 1.8D | 2.2D |
| | Overall bandwidth measured with reference to peak positive and negative velocity | 1.91U _{in} | 1.05U _{in} |
| | Overall downstream velocities approaching main velocity | Early | Late |
| | Fluctuation of velocities with respect to variation of each Reynolds number | Low Reynolds number | Large |
| High Reynolds number | | Small | Small |
| Wave-3 | Region negative velocities behind the bluff body | 2.5D | 1D |
| | Overall bandwidth measured with reference to peak positive and negative velocity | 1.46U _{in} | 0.5U _{in} |
| | Overall downstream velocities approaching main velocity | Early | Late |
| | Fluctuation of velocities with respect to variation of each Reynolds number | Low Reynolds number | Small |
| High Reynolds number | | Large | Small |

